

# PROBLEMS IN HIGH ENERGY ASTROPHYSICS

PAOLO LIPARI

*INFN, sez. Roma “La Sapienza”*

E-mail: paolo.lipari@roma1.infn.it

## ABSTRACT

In this contribution we discuss some of the main problems in high energy astrophysics, and the perspectives to solve them using different types of “messengers”: cosmic rays, photons and neutrinos.

## 1. Introduction

The birth of high energy astrophysics can be traced to nearly a century ago, when the balloon flights of Victor Hess established that a form of ionizing radiation, that was soon given the name of “cosmic rays”, was arriving from outer space. Soon it was demonstrated that these “rays” are in fact ultrarelativistic charged particles, mostly protons and fully ionized nuclei<sup>a</sup>, with a spectrum that extends to extraordinary high energies. The existence of a large flux of ultrarelativistic particles arrived completely unexpected, and its origin remained a mystery that only now is beginning to be clarified. The main reason for this very long delay in developing an understanding of this important physical phenomenon is that cosmic rays (CR) do not point to their production sites, because their trajectory is bent by the magnetic fields that permeates both interstellar and intergalactic space.

Today we know that our universe contains several classes of astrophysical objects where non-thermal processes are capable to accelerate charged particles, both leptons ( $e^\mp$ ) or hadrons (protons and nuclei), to very high energy. These relativistic particles, interacting inside or near their sources, can produce photons, and (in case of hadrons) neutrinos that then travel in straight lines allowing the imaging of the sources. At the highest energy also the magnetic bending of charged particles can become sufficiently small to allow source imaging. A detailed study of the “high energy universe” can therefore in principle be performed using three different “messengers”: photons, neutrinos and the cosmic ray themselves. This “multi-messenger” approach is still in its infancy, but has the potential to give us deep insights about the sites and physical mechanisms that produce these very high energy particles.

Many of the proposed (or detected) acceleration sites are also associated with the violent acceleration of large macroscopic masses (one example is Gamma Ray Bursts), and therefore a fourth “messenger”: gravitational waves has the potential to give very

---

<sup>a</sup> Electrons have a steeper energy spectrum and constitute a fraction of only few percent of the flux; small quantities of positrons and anti-protons are also present.

important and complementary information about these astrophysical environments.

## 2. The Cosmic Ray Spectrum

The spectrum of hadronic CR observed at the Earth is shown in fig. 1, it spans approximately 11 order of magnitude in energy up to  $E \sim 10^{20}$  eV. The CR spectrum is remarkably smooth and can be reasonably well approximated by a power law form ( $\phi \propto E^{-\alpha}$ ) with a nearly constant slope. The most prominent spectral features are the “Knee” at  $E \simeq 3 \times 10^{15}$  eV, where the spectrum steepens from a slope  $\alpha \simeq 2.7$  to  $\alpha \simeq 3$ , and the “Ankle” at  $E \simeq 10^{19}$  eV, where the spectrum flattens to have again the slope  $\alpha \simeq 2.7$ . At  $E \sim 6 \times 10^{19}$  eV there is now clear evidence (from the HiRes<sup>1)</sup> and Auger<sup>2)</sup> collaborations) of a sharp steepening of the spectrum. Such a spectrum suppression had been predicted more than 40 years by Greisen, Zatsepin and Kuzmin<sup>3)</sup> (GZK) as the consequence of the interactions of high energy particles with the photons of the 2.7 Kelvin Cosmic Microwave Background Radiation (CMBR). The non observation of this effect generated intense interest and an abundant literature. The observed spectrum suppression is consistent with the shape predicted for the GZK mechanism (pion production in  $p\gamma$  interactions), but other dynamical explanations are possible including fragmentation of heavy nuclei, or an intrinsic high energy cutoff in the CR sources. An additional (less evident) steepening of the spectrum (with

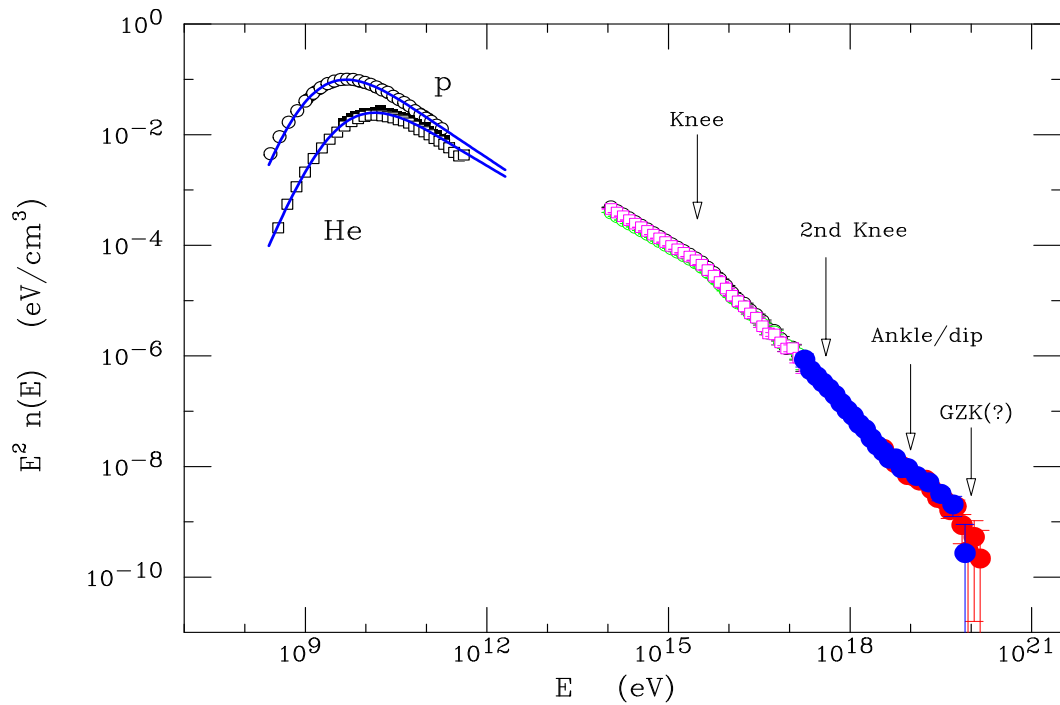


Figure 1: General structure of the CR energy spectrum plotted in the form  $\phi(E) E^2$  versus  $\log E$

the slope increasing from  $\alpha \simeq 3$  to approximately 3.3) the so called “2nd–Knee” at  $E \sim 4 \times 10^{17}$  eV has recently emerged as potentially very significant. Explanations for the origin of the “Knee”, and the “2nd–Knee” and the “Ankle” are still disputed, and are considered as of central importance for an understanding of the CR.

It is now known<sup>4)</sup> that most of the CR that we observe near the Earth are “galactic”, they are produced by sources inside our Galaxy, and are confined by galactic magnetic fields to form a “bubble” (or “halo”) around the visible disk of the Milky Way with a form and dimension that are still the object some dispute. Extragalactic space should also be filled by a (much more tenuous) gas of CR, produced by the ensemble of all sources in the universe during their cosmological history.

All galaxies (including ours) should be sources of CR, as the particles that “leak out” of magnetic confinement are injected into extragalactic space, however it is possible (and predicted) that there are additional sources of extragalactic CR that are not normal galaxies like our Milky Way, but special objects like for example Active Galactic Nuclei (AGN) or colliding galaxies. The extra–galactic component is expected to have a harder energy spectrum, and should emerge above the foreground of galactic CR at sufficiently high energy. The determination of a “transition energy” that marks the point where the extragalactic CR component becomes dominant is a very important problem (see discussion in section 4.3).

### 3. Galactic Cosmic Rays

Ultrarelativistic charged particles produced inside our Galaxy remain trapped by the galactic magnetic field, that has a typical strength<sup>b</sup>  $B \sim 3 \mu\text{Gauss}$ . The Larmor radius of a charged particle in a magnetic field is:

$$r_{\text{Larmor}} = \frac{E}{Z e B} \simeq \frac{1.08}{Z} \left( \frac{E}{10^{18} \text{ eV}} \right) \frac{\mu\text{Gauss}}{B} \text{ kpc} \quad (1)$$

(one parsec is  $3.084 \times 10^{18}$  cm, or approximately 3 light years). Magnetic confinement becomes impossible when the gyroradius is comparable with the linear dimensions of the Galaxy. This corresponds to energy:

$$E \gtrsim Z e B R_{\text{Halo}} \simeq 2.7 \times 10^{19} Z \left( \frac{B}{3 \mu\text{Gauss}} \right) \left( \frac{R_{\text{Halo}}}{10 \text{ Kpc}} \right) \quad (2)$$

Most CR particles have much lower energy and a gyroradius that is much smaller than the galactic size. The motion of these particles can be well approximated as a diffusive process controlled by the random component of the galactic field. The time needed

---

<sup>b</sup> The magnetic field receives approximately equal contributions from a “regular” component (that in the galactic plane has field lines that run parallel to the spiral arms) and an irregular component generated by turbulent motions in the interstellar medium. Our knowledge of the field has still significant uncertainties and is very important fields of research.

for a CR particles to diffuse out of the galactic halo depends on its rigidity (indicated in the following for ultrarelativistic particles as  $E/Z$ ). In zero order approximation (a spherical homogeneous halo) the confinement time of a CR can be estimated as:

$$\tau\left(\frac{E}{Z}\right) \simeq \frac{R_{\text{Halo}}^2}{D(E/Z)} \quad (3)$$

where  $R_{\text{Halo}}$  is the halo radius and  $D(E/Z)$  is a rigidity dependent diffusion coefficient. An important consequence is that (assuming stationarity) the population  $N_A(E)$  of CR of type  $A$  and energy  $E$  in the Galaxy is:

$$N_A(E) \simeq Q_A(E) \tau(E/Z) \quad (4)$$

where  $Q_A(E)$  is the injection rate and  $\tau(E/Z)$  is the (rigidity dependent) residence time. Therefore the observed CR spectrum has not the same energy distribution of the particles near their sources, but is distorted and steepened by confinement effects:

The determination of the shape of the “source spectrum”  $Q(E)$  and of the length and rigidity dependence of the confinement time are obviously important problems. A powerful method is the measurement of the spectra of “secondary nuclei” (such as Lithium, Beryllium and Boron) in the CR. These nuclei are very rare in normal matter, but they are relatively abundant in the CR flux, because they are produced in the spallation of parent nuclei such as Carbon and Oxygen, a process where the nuclear fragments maintain the same velocity and therefore the same energy per nucleon as the incident nucleus. The energy spectrum of secondary nuclei is expected to be proportional to the square of the confinement time (its own, and of the parent particle). The measurements<sup>5)</sup> indicate that while “primary” nuclei have spectra  $\propto E^{-2.7}$ , secondary nuclei have steeper spectra  $\propto E^{-3.3}$ . The conclusion is that the confinement time decreases with rigidity as  $\tau \propto E^{-\delta} \simeq E^{-0.6}$ , and therefore the injection spectrum of CR at their sources has a slope  $\alpha_{\text{inj}} \simeq \alpha_{\text{obs}} - \delta \simeq 2.1$ . The absolute value of the confinement time can be estimated from the relative amounts of secondary and primary nuclei in the CR flux, with additional information obtained studying the abundance of unstable nuclear isotopes<sup>6)</sup> with appropriate lifetime (in particular the nucleus Beryllium-10 with a half like of 1.5 Million years) and is of order of 10 million years for a rigidity of a few GeV.

The power law rigidity dependence ( $\tau \propto E^{-\delta}$ ) of the confinement time, and of the diffusion coefficient ( $D \propto E^\delta$ ) is not unexpected, because for a turbulent magnetic field one predicts a power law form for the diffusion coefficient with a slope that is a function of the power spectrum of the field irregularities. For the theoretically favoured Kolmogorov turbulence one expects  $\tau(E) \propto E^{-1/3}$ . This results would imply a steeper injection spectrum  $\propto E^{-2.37}$ . The discrepancy between this theoretical

prediction and data is still under discussion.

### 3.1. The “SuperNova Paradigm” for galactic Cosmic Rays

A confinement time of a few million years is in fact very short with respect to the age of the Galaxy, and therefore CR must continuously be produced in our Galaxy (that is in a stationary state with approximately equal CR injection and loss). The power of the ensemble of CR sources in the Milky Way can be estimated as the ratio between the total energy of CR in the Galaxy divided by their average confinement time:

$$L_{\text{cr}}^{\text{Milky Way}} \simeq \frac{\rho_{\text{cr}}(x_{\odot}) V_{\text{eff}}}{\langle \tau_{\text{cr}} \rangle} \simeq 2 \times 10^{41} \left( \frac{\text{erg}}{\text{s}} \right) \quad (5)$$

For this numerical estimate we have used a local CR energy density<sup>c</sup>  $\rho_{\text{cr}}(\vec{x}_{\odot}) = 1.6 \text{ eV/cm}^3$ , an effective volume of  $170 \text{ Kpc}^3$  and a average confinement time of 20 Million years. This surprisingly large power requirement (approximately 50 million solar luminosities), is a very important constraint for the identification of the galactic CR sources. In fact, simply on the basis of this energy condition SuperNova (SN) explosions were proposed<sup>7,8)</sup> as the most likely CR source. The average kinetic energy of a SN ejecta is of order  $L_{\text{kin}} \simeq 1.6 \times 10^{51} \text{ erg}$  (this corresponds to the kinetic energy of 10 solar masses traveling at  $v \simeq 4000 \text{ Km/s}$ ). For a SN rate in our Galaxy of order every  $(30 \text{ years})^{-1}$  the power associated to all SN ejections is then  $L_{\text{SNR}}^{\text{kin}} \simeq 1.7 \times 10^{42} \text{ erg/s}$ , and it is therefore possible to regenerate the Milky Way CR if approximately 10–20% of the kinetic energy of the ejecta is converted into a population of relativistic particles.

In addition to these energy balance considerations, in the 1970’s a dynamical argument emerged in favour of the SuperNova hypothesis, when it was understood (see Drury<sup>9)</sup> for a review) that the spherical shock waves produced in the interstellar medium by the (supersonically moving) SN ejecta can provide the environment where particles, extracted from the tail of a thermal distribution, are accelerated up to very high energy generating a power law spectrum with a well defined slope of order  $\alpha \simeq 2 + \epsilon$  with  $\epsilon$  a small positive number. That is precisely the injection spectrum needed to generate the observed CR.

The basic concept behind this theory is an extension of the ideas developed by Enrico Fermi<sup>10)</sup>, who in 1949 made the hypothesis that the acceleration of cosmic rays is a stochastic process, where each CR particle acquires its high energy in undergoing many collision with moving plasma clouds. The clouds carry (in their own rest frame) turbulent magnetic fields and act as ‘magnetic mirrors’ imparting on average

---

<sup>c</sup> The estimate of the CR energy density is of the same order of magnitude of the energy density of the galactic magnetic field (for  $B \simeq 3 \mu\text{Gauss}$  one has  $\rho_B = B^2/(8\pi) \simeq 0.22 \text{ eV/cm}^3$ ). This is not a coincidence, and has a transparent dynamical explanation. The galactic magnetic field is mostly generated by electric currents transported by the CR, while the CR themselves are confined by  $\vec{B}$ , and therefore the two quantities are close to equilibrium.

a positive “kick” to the scattering particle with  $\langle \Delta E \rangle / E \propto \beta^2$  (with  $\beta$  the cloud velocity). It is easy to see that this process generates a power law spectrum, with higher energy particles having performed a larger number of collisions.

The crucial new element introduced in the 1970’s is the presence of the shock wave. Charged particles are now accelerated scattering against magnetic (in the plasma rest frame) irregularities present both upstream and downstream of the shock front that act as Fermi’s clouds, or converging magnetic mirrors. The new geometry allows a more efficient acceleration [ $(\langle \Delta E \rangle / E)_{\text{crossing}} \propto \beta_{\text{shock}}$ ] and the (mass, momentum and energy conservation) constraints of the fluid properties across the shock determine the slope ( $\alpha \simeq 2 + \epsilon$ ) of the accelerated particle spectrum.

This mechanism (diffusive acceleration in the presence of shock waves) can operate every time that one has a shock wave in an astrophysical fluid. The spherical blast waves of SN ejecta are one example of this situation but several other are known to exist. In fact shocks are generated every time that macroscopic amounts of matter move at supersonic speed. Particularly interesting case are the jets emitted by Gamma Ray Bursts, by accreting Black Holes of stellar mass (microQuasars) or supermassive (Active Galactic Nuclei). In all these objects there is in fact evidence for particle acceleration.

The “SuperNova Paradigm” has a simple and very important implication: in the vicinity of young SuperNova Remnant (SNR) one should find a population of relativistic hadrons (protons and nuclei) with a spectrum close to the injection one ( $E^{-(2+\epsilon)}$ ) and a total energy of order  $\sim 0.2 \times 10^{51}$  erg. These relativistic particles can interact with the interstellar medium around the SN producing neutral and charged pions that then decay generating photons and neutrinos with a spectrum that to a good approximation follows the same power law of the parent proton spectrum. Describing the relativistic proton population as  $N_p(E) \simeq K_p E^{-\alpha}$ , and approximating the confinement volume as homogeneous and with density  $n_T$ , the rate of emission of photons and neutrinos is approximately:

$$\dot{N}_{\gamma(\nu)}(E) = K_p (c \sigma_{pp} n_T) Z_{p \rightarrow \gamma(\nu)}(\alpha) E^{-\alpha} \quad (6)$$

where  $\sigma_{pp}$  is the  $pp$  interaction cross section<sup>d</sup> and  $Z_{p \rightarrow \gamma(\nu)}$  are adimensional proportionality factors. For a proton spectrum  $\propto E^{-2}$  that has equal energy per decade of energy the  $Z_{p \rightarrow \gamma(\nu)}$  factors are well approximated by the (approximately energy independent) fraction of the energy of the interacting protons that goes into photons (or neutrinos), with  $Z_{p\gamma} \sim Z_{p\nu} \sim 0.15$ . Using the theoretically expected slope  $\alpha \simeq 2$ , fixing the constant  $K_p$  by the total energy contained in the relativistic particles, assuming a spectrum extending in the interval  $[E_{\text{min}}, E_{\text{max}}]$ , a source at a distance  $d$

---

<sup>d</sup>For simplicity we use a notation that indicates only the dominant components for both the CR and the target medium.

and integrating above  $E_{\text{th}}$  the photon (or neutrino) integrated flux at the Earth is:

$$\begin{aligned}\Phi_{\gamma(\nu)}(E_{\text{th}}) &\simeq \frac{(c \sigma_{pp} n_T)}{4 \pi d^2} \frac{E_{\text{cr}}^{\text{tot}}}{\ln(E_{\text{max}}/E_{\text{min}})} \frac{Z_{p \rightarrow \gamma(\nu)}}{E_{\text{th}}} \\ &\simeq 0.9 \times 10^{-11} \left(\frac{\text{Kpc}}{d}\right)^2 \left(\frac{n_T}{\text{cm}^{-3}}\right) \left(\frac{E_{\text{cr}}^{\text{tot}}}{10^{50} \text{ erg}}\right) \left(\frac{\text{TeV}}{E_{\text{th}}}\right) \text{ cm}^{-2} \text{ s}^{-1}\end{aligned}\quad (7)$$

with  $d$  the source distance. Equation (7) is a key prediction of the ‘‘SNR paradigm’’ for the acceleration of the bulk of cosmic rays that can be tested with photon observations in the GeV/TeV regions, and soon also with neutrino telescopes.

In 2004<sup>11)</sup> the HESS TeV Cherenkov telescope observed the SuperNova Remnant RX J1713.7-3946<sup>e</sup> as a very bright source of TeV photons. The property of the photons from this source, taking into account our knowledge of the density of the environment around the object are consistent<sup>12)</sup> with the expectation of the ‘‘SNR paradigm’’ for galactic cosmic rays.

Several other young SNR have also been detected with TeV photons (this includes the detection of Cassiopea A<sup>13)</sup>), while for other objects one has only upper limits. These observation of SNR in high energy photons gives support to the ‘‘SNR paradigm’’ for CR acceleration (for a more critical view of the situation see<sup>14)</sup>). This conclusion is however not unambiguous; also for the best candidate source RX J1713.7-3946 a ‘‘leptonic origin’’ of the radiation (inverse Compton of relativistic  $e^\mp$  on the radiation fields around the SN) cannot be entirely excluded.

It is remarkable that the neutrino flux that should accompany the photon flux in case of a ‘‘hadronic’’ origin ( $\pi^0 \rightarrow \gamma\gamma$  decay, accompanied by  $\pi^+ \rightarrow \mu^+ \nu_\mu \rightarrow (e^+ \nu_e \bar{\nu}_\mu) \nu + \mu$  chain decay) is detectable, at the level of few neutrino induced up-going muon events per year, in a  $\text{Km}^3$  size neutrino telescope placed in the northern hemisphere. Photon observations in the GeV region with detectors on satellites (Agile and GLAST) have also the potential to test the ‘‘SuperNova paradigm’’ for CR production.

### 3.2. The ‘‘Knee’’, and the maximum acceleration energy

The mechanism of diffusive particle acceleration generates a power law spectrum only up to a finite maximum energy  $E_{\text{max}}$ . This maximum energy is determined by the product of the acceleration rate times the total time available for the acceleration. Simple considerations allow to estimate  $E_{\text{max}} \simeq Z e B R \beta_{\text{shock}}$  where  $B$  is the typical strength of the magnetic field,  $R$  the linear dimension of the acceleration site and  $\beta_{\text{shock}}$  the shock velocity. Note that this estimate is more stringent than a simple

---

<sup>e</sup> An object discovered in X-rays by the ROSAT instrument and then associated, with a very high degree of confidence, to a supernova observed and recorded by chinese astronomers in the year 393 of the current era.

magnetic containment condition by a factor  $\beta_{\text{shock}} < 1$ . Substituting values that are relevant for a SNR one finds:

$$E_{\text{max}} \simeq Z e B R \beta_{\text{shock}} \simeq 0.4 \times 10^{14} \text{ eV } Z \left( \frac{R}{5 \text{ pc}} \right) \left( \frac{B}{3 \mu\text{Gauss}} \right) \left( \frac{\beta_{\text{shock}}}{0.03} \right) \quad (8)$$

This estimated maximum energy is much smaller than the highest observed energies, and therefore it is clear than other type(s) of CR sources must exist.

The estimate (8) is however not too dissimilar from the “Knee” energy (at  $E \simeq 3 \times 10^{15}$  eV, and it has been suggested that the “Knee structure” marks in fact the maximum energy for *proton* acceleration in SNR. The apparent smooth behaviour of the spectrum above the knee could hide a succession of cutoffs with increasing energies ( $E_{\text{max}}^Z = Z E_{\text{max}}^p$ ) for heavier nuclear species. In this model the SNR spectrum would extend up to the maximum energy for iron with  $E_{\text{max}}^{\text{iron}} \simeq 0.8 \times 10^{17}$  eV. The key prediction here is the gradual change (with increasing  $\langle A \rangle$ ) CR composition above the knee, or more precisely a set of different “knees” at identical rigidity, and therefore scaling in energy proportionally to the electric charge  $Z$ . Unfortunately the measurement of particle mass in Extensive Air Showers in the region of the knee<sup>f</sup> are not easy and suffer from significant uncertainties in the modeling of the shower (see below in section 6). The data of Cascade<sup>22)</sup> and other experiment are (with large errors) roughly consistent with this idea.

Equation (8) for the maximum energy is valid in general, for all astrophysical environments where shocks are present in a diffusive medium, and setting  $\beta_{\text{shock}} = 1$  the equation simply gives a very general condition for containment in the source. Since one observes particles with energy up to  $10^{20}$  eV, the acceleration of these particles requires sources with a sufficiently large  $B R$  product, that is sources with a sufficiently strong magnetic field and sufficiently extended to satisfy condition (8). This point has been stressed by Michael Hillas<sup>23)</sup> that initiated a systematic study of all possible astrophysical environments that are possible candidates for ultra high energy acceleration on the basis of equation (8). The bottom line of this analysis is that this very simple constraint is very “selective” and only few objects are viable for acceleration up to  $E \sim 10^{20}$  eV. The main candidates are Active Galactic Nuclei, and the jet-like emission associated with the Gamma Ray Bursts.

### 3.3. Alternative Models

A possible alternative to the SNR paradigm is the “cannon ball model” of Dar and De Rujula<sup>15)</sup>. In this model the Energy source for the production of CR is ultimately the same as in the SNR paradigm, and is the gravitational binding energy released during the collapse of massive stars at the end of their evolution, but the dynamics

---

<sup>f</sup> The best method is the simultaneous measurement of the electromagnetic and muon component of the shower at ground level.

of CR acceleration is deeply different. In the cannon ball model the explosion due to a gravitational collapse produce in most of perhaps all of the cases not only a quasi-spherical mass ejection with an initial (non-relativistic) velocity of order  $10^4$  Km/s, but also the emission along the rotation axis of the collapsing star of “blobs” of ordinary matter each having a mass of order  $10^{26}$  grams and an extraordinary Lorentz factor of order  $\Gamma = 1000$ ; the “cannon balls” emission, according to the authors is responsible for most of the Gamma Ray Bursts<sup>16)</sup>, with a mechanism that differs from the often discussed “Fireball model”<sup>17,18)</sup>. Cosmic rays are accelerated by the collisions of the cannon balls while they decelerates slowly colliding with the interstellar medium.

In this work we do not have the space to discuss critically this model, see reference<sup>29)</sup> for criticism (and the authors’ response<sup>19)</sup>).

#### 4. Extragalactic Cosmic Rays

Most ultrarelativistic particles injected in extragalactic space have negligible interaction probability, and only lose energy because of the universal redshift effects. The important exceptions are those particles that have a sufficiently high energy to interact with the abundant photons of the Cosmic Microwave Background Radiation (CMBR). For protons one has to consider two important thresholds associated to pair production ( $p + \gamma \rightarrow p + e^+e^-$ ):

$$E_{\text{th}}^{e^+e^-} \sim \frac{2m_e m_p}{10 T_\gamma} \simeq 4 \times 10^{17} \text{ eV} \quad (9)$$

and pion production ( $p + \gamma \rightarrow N + \pi$ ):

$$E_{\text{th}}^\pi \sim \frac{m_\pi m_p}{10 T_\gamma} \simeq 6 \times 10^{19} \text{ eV} \quad (10)$$

For heavy nuclei one has to consider the photodisintegration reactions with threshold (related to the process  $A + \gamma \rightarrow (A - 1) + N$ ):

$$E_{\text{th}}^{\gamma A} \sim \frac{A m_p \varepsilon_B}{10 T_\gamma} \simeq 3 \times 10^{18} A \left( \frac{\varepsilon_B}{8 \text{ MeV}} \right) \text{ eV} \quad (11)$$

where  $\varepsilon_B$  is the binding energy of the displaced nucleon. Note that the threshold energies for protons and iron nuclei ( $A \simeq 56$ ) differ by a factor 2-3. Particles above the thresholds (9) and (10) lose rapidly energy cannot propagate only for a cosmologically short time. This results in a strong flux suppression.

The (space) average extragalactic density  $\langle n_a(E) \rangle$  of particle type  $a$  (for example protons, or neutrinos) can be calculated integrating the source emission over the entire history of the universe, taking also into account the effects of energy loss or absorption. A general expression for the average particle density is:

$$\langle n(E) \rangle = \int_0^\infty dt \int dE_g q(E_g, t) P(E, E_g, t) \quad (12)$$

where the double integral is over the emission time and the emission energy,  $q(E, t)$  is the (space averaged) emissivity for the particle considered (that is the number of particles emitted per unit of time, comoving volume and energy at universal time  $t$ ), and  $P(E, E_g, t)$  is the probability that a particle generated with energy  $E_g$  at time  $t$  survives until the present epoch with energy  $E$ .

Expression (12) can be simplified if one makes the assumption that the energy loss is a continuous deterministic process, and the probability  $P$  can be approximated with the expression:

$$P(E, E_g, t) = \delta[E - E_g(E, t)] \quad (13)$$

where the function  $E_g(E, t)$  is the energy of a particle observed now with energy  $E$  after propagation backward in time to time  $t$ . This approximation is essentially perfect for neutrinos, and also sufficiently accurate for protons.

One can rewrite equation (12) changing the integration variable from  $t$  to the redshift  $z$  with the Jacobian factor:

$$\frac{dt}{dz} = -\frac{1}{H(z)(1+z)} \quad (14)$$

where  $H(z)$  the Hubble constant at the epoch redshift  $z$ :

$$H(z) = H_0 \sqrt{\Omega_m (1+z)^3 + \Omega_\Lambda + (1 - \Omega_\Lambda - \Omega_m) (1+z)^2}, \quad (15)$$

and performing the integration over  $E_g$  using the delta function. The result can be written in the form:

$$\langle n(E) \rangle = \frac{1}{H_0} q(E, 0) \zeta(E) \quad (16)$$

where  $\zeta(E)$  is an adimensional ‘‘shape factor’’:

$$\zeta(E) = \int_0^\infty dz \frac{H_0}{H(z)} \frac{1}{(1+z)} \frac{q[E_g(E, z)]}{q(E, 0)} \frac{dE_g(E, z)}{dE} \quad (17)$$

The expression (16) has a transparent physical interpretation:  $q(E, 0)$  tells us how many particles of energy  $E$  are injected per unit time and unit volume in the present universe, multiplying by the Hubble time  $H_0^{-1}$  we obtain a first order estimate of the present density, and the ‘‘shape factor’’ contains all complications related to the expansion of the universe, the cosmological evolution of the sources, and the energy losses of the particle considered.

#### 4.1. The proton extragalactic spectrum

We can now use expression (16) to compute the extragalactic proton flux assuming that it is related to the space averaged density by the simple relation<sup>g</sup>

$$\phi_p(E) = \frac{c}{4\pi} \langle n_p(E) \rangle = \frac{c}{4\pi} \frac{1}{H_0} q(E, 0) \zeta(E) \quad (18)$$

---

<sup>g</sup>In general the effects of the magnetic field, and of the ‘‘granularity of the sources can result in modification of this assumption.

The simplest assumption for the injection is a power law form:  $q(E) = q_0 E^{-\alpha}$  that depends only on two parameters, the slope  $\alpha$  and the absolute normalization. The calculation of the flux has three obvious steps, the first is the calculation of the evolution of the proton energy with redshift; the second is the calculation of the shape factor  $\zeta(E)$  according to equation (17), and finally one can use equation (18).

The results of a numerical calculation of  $E_g(E, z)$  are shown in fig. 2. The different curves correspond to the “backward in time” evolution of the energy of protons detected “now” with  $E$  between  $10^{17}$  eV and  $10^{22}$  eV. For each energy  $E$  one finds (at a certain redshift  $z$ ) a sort of “photon wall”, where the  $E(z)$  starts to grow faster than an exponential. Clearly at this critical redshift the universe (filled with a hotter and denser radiation field) has become opaque to the propagation of the protons. Note

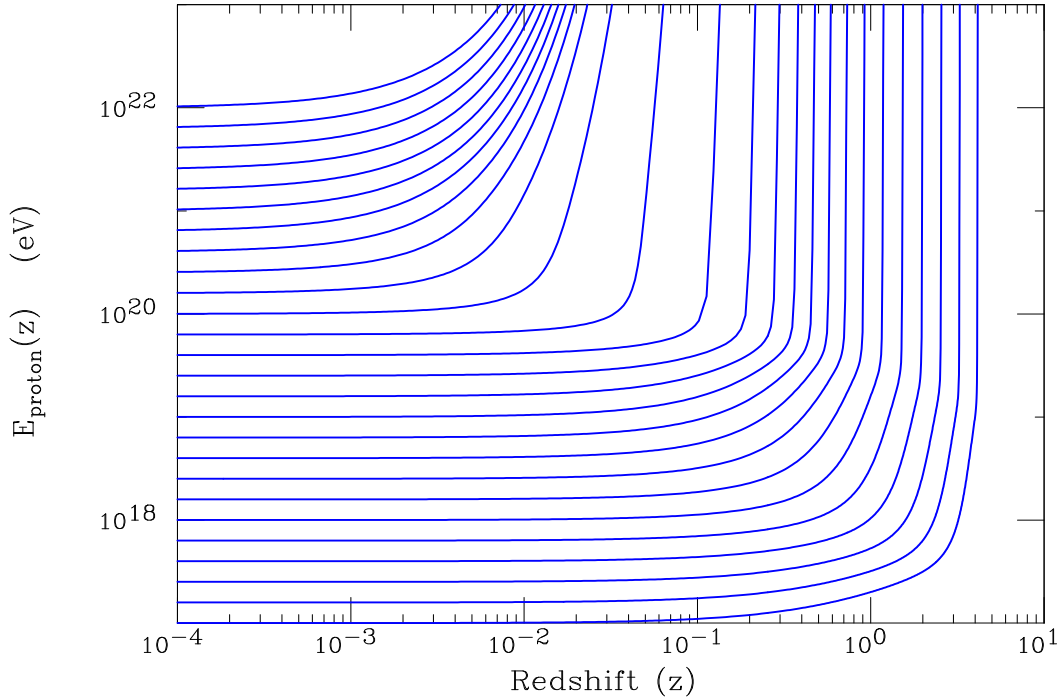


Figure 2: Redshift (time) dependence of the energy of protons observed with different final energy at the present epoch.

that the time evolution of the energy of a proton is completely independent from the structure and intensity of the magnetic fields, because a magnetic field can only bend the trajectory of a particle and the target radiation field is isotropic<sup>h</sup>.

The result of the calculation of the “shape factor”  $\zeta(E)$  for a power law injection is shown in fig. 3. It is important to note that the function  $\zeta(E)$  has a non trivial energy dependence, and while the injection spectrum is a smooth power law will show

---

<sup>h</sup>Clearly in this case the redshift maintains its one to one correspondence with the time of emission of the particle, but loses its simple relation with the space distance of the particle source.

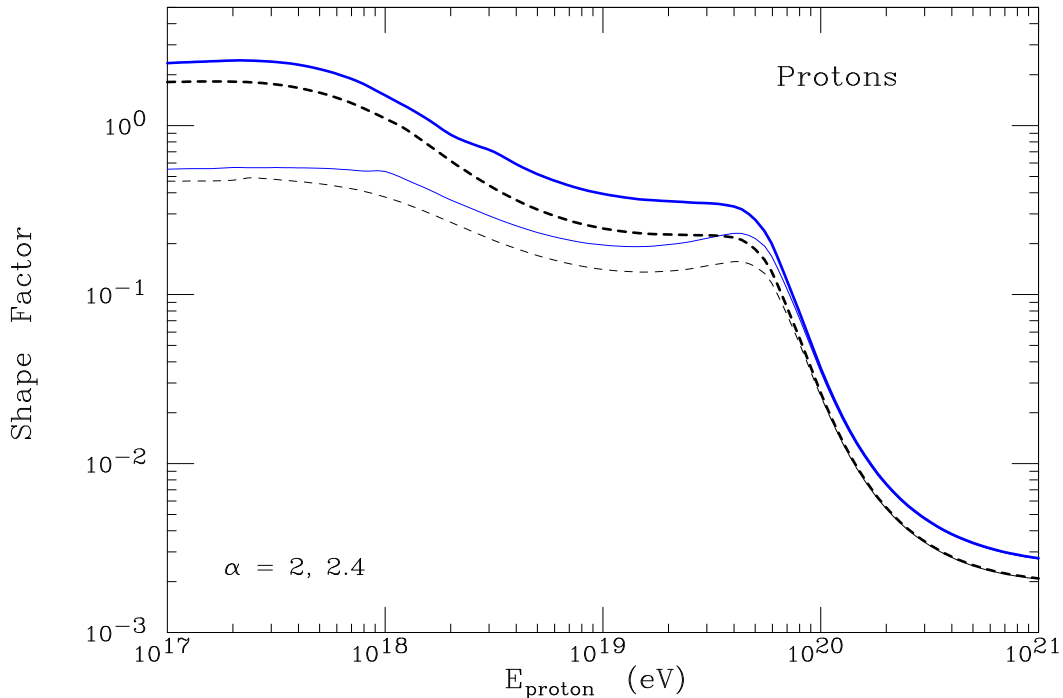


Figure 3: Shape factor  $\zeta(E)$  for protons, calculated for a power injection with slope  $\alpha = 2.0, 2.2, 2.4$  and  $2.6$ . The solid lines are calculated for a constant value of the source power density, while the dashed lines assume for  $\mathcal{L}_p(z)$  the redshift dependence shown estimated by Ueda <sup>24</sup>) for the X-ray luminosity of AGNs.

some structure, the “imprints” of the energy loss processes (pair and pion production) of the protons. For energy  $E \ll E_{\text{th}}^{e^+e^-}$ , only adiabatic (redshift) energy losses are significant, and in this case the the shape factor  $\zeta(E)$  tends to a constant value:

$$\zeta \rightarrow \int_0^\infty dz \frac{H_0}{H(z)} (1+z)^{-\alpha} \frac{\mathcal{L}(z)}{\mathcal{L}_0} \quad (19)$$

( $\mathcal{L}(z)/\mathcal{L}_0$  is the cosmological evolution of the source luminosity). Accordingly, the power law injection results in an observable flux that is a power law of the same slope. At higher energy the energy losses due to the pair production and pion production thresholds (equations (9) and (10)) leave their “marks” on the shape of the energy spectrum.

The results of the calculations for the observable flux are shown in fig. 4 and fig. 5. The calculations were performed with different slopes of the injection power law  $\alpha = 2.0, 2.2, 2.4$  and  $2.6$ , and with two different assumptions for the evolution of the cosmic sources, a constant injection, and evolution equal to the one estimated in<sup>24</sup>) for the AGN hard X-ray emission. The normalization of the calculation is chosen in order to have a good fit to the observed data in the very high energy region. Some comments about the results shown in fig. 4 are in order:

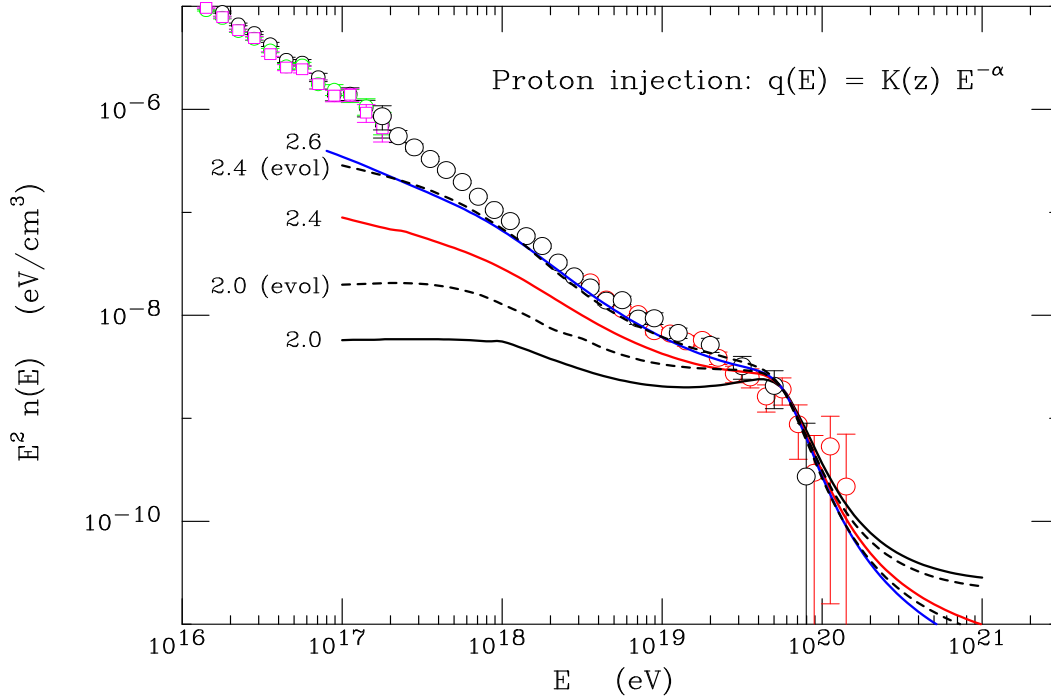


Figure 4: Extragalactic proton spectrum calculated for a power law injection with different slopes  $\alpha$ , for no-evolution of and with the evolution of<sup>24)</sup>. The data points are from the Tibet array<sup>27)</sup> and the HiRes detector<sup>1)</sup>.

(i) The shape of the observed flux above  $E \gtrsim 5 \times 10^{19}$  eV is consistent with the presence of the suppression predicted by GZK<sup>3)</sup>. The implication of this point are discussed below in section 4.2.

(ii) The shape of the calculated spectrum is determined by the slope  $\alpha$  of the injection spectrum and also by the assumptions about the redshift dependence of the injection. Actually this redshift dependence is of small importance for  $E \gtrsim 5 \times 10^{19}$  eV because the lifetime of a very high energy particle is brief and they do not probe deeply into the past history of the universe. For lower energy the inclusion of source evolution is significant. Lower energy particles can arrive from a more distant past when the emissivity was higher, and therefore, for the same shape of the injection, the inclusion of source evolution results in a softer spectrum. As a rule of thumb, including for the injection the redshift dependence of the AGN luminosity (or also of the stellar formation rate) has an effect similar to the softening of the injection spectrum of order  $\Delta\alpha \simeq 0.2$ .

(iii) It is remarkable that if one choses an injection spectrum with a shape  $\propto E^{-2.6}$  and no source evolution (or a source  $\propto E^{-2.4}$  with cosmic evolution) with appropriate normalization, the calculated flux can provide a good match to the data in the entire region from  $E \simeq 10^{18}$  eV up to the highest energies. The possible implications of this result are discussed below in section 4.3.

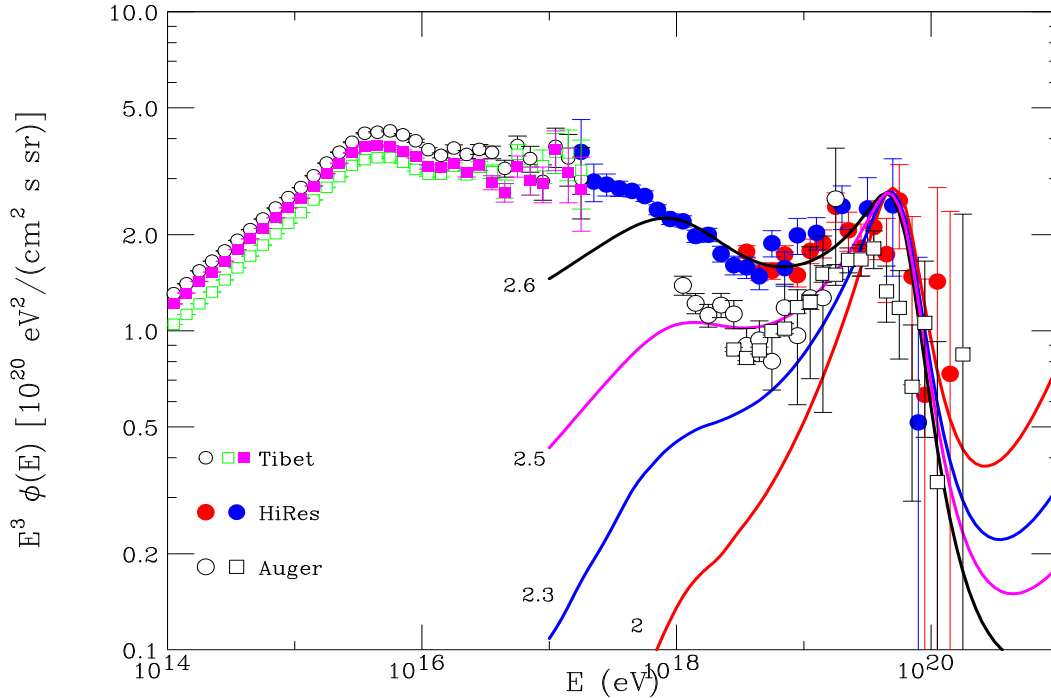


Figure 5: High energy CR spectrum. For clarity only the data of the Tibet array<sup>27)</sup> (below  $E \simeq 10^{17}$  eV), HiRes<sup>1)</sup> and Auger<sup>2)</sup> (at higher energy) are shown. The spectrum is plotted in the form  $\phi(E) E^3$  versus  $\log E$ . One can note the different energy scales for the HiRes and Auger experiment. The Tibet data points are calculated using three different interaction models for the reconstruction of the shower energy. The lines describe the shape of an extragalactic components with injection spectrum  $E^{-\alpha}$  and normalized to fit the high energy data.

#### 4.2. The “GZK controversy”

For several years the “dominant question” in CR physics has been the possible existence of a large flux of particles with energy larger than  $10^{20}$  eV. To solve this very surprising result two main arguments have been proposed. One possibility is the existence of an additional source of particles of extremely high energy from the decay of super-heavy (mass of order of the GUT mass  $M_{\text{GUT}} \simeq 10^{25}$  eV). A second possibility is the existence of violation of the Lorentz invariance. The process  $p\gamma \rightarrow N\pi$  that is at the basis of the expected suppression of the proton flux is in fact studied in the laboratory mostly in the  $p$  rest frame, while for CR it is relevant in a frame where the  $p$  has a Lorentz factor  $E_p/m_p \sim 10^{11}$ . One can therefore speculate that “small” violations of the Lorentz invariance could suppress the cross section for high energy CR. Ultra High Energy Cosmic Rays therefore offered the exciting possibility of being the key observational field for the exploration for new physics.

The new results of the HiRes<sup>1)</sup> and Auger<sup>2)</sup> collaborations demonstrating the

existence of a suppression of the CR flux at  $E \simeq 6 \times 10^{19}$  eV have however very significantly changed the “scientific landscape” around the field. The phenomenological motivations for “exotic physics” in UHECR have essentially disappeared. Of course, the theoretical arguments behind the existence of supermassive topological defects as relics from the early universe, and (perhaps more controversially) of possible violations of the Lorentz invariance remain in existence, and therefore UHECR can be used to set limits, or look for hints of these phenomena. However the field of UHECR has now returned to its status as an “astrophysical problem”, where the main questions is to establish what are the sources of these ultrarelativistic particles, and what are the physical processes responsible for the acceleration<sup>i</sup>.

Does this new situation makes the study of CR less interesting? In a certain sense the answer is obviously yes. The significance of the “exotic physics” for the UHECR would clearly be of truly revolutionary significance. On the other hand the astrophysics of CR, or more in general study of the origin of the different forms of high energy radiation remain a field of *fundamental* importance.

The development of fundamental Science has historically always been intimately connected with the discovery and understanding of astrophysical objects. Steps in this remarkable history have been the understanding of: the structure and dynamics of the solar system; the source of energy in the Sun and the stars; the quantum mechanical effects that sustain White Dwarf stars; the formation of neutron stars and their connection with SuperNova explosions.

The sources of the high energy radiation in the universe (some of which are still undiscovered) are very likely (together with the early universe) the most “extreme” environments where we can perform the most stringent tests for physical laws in conditions that are often simply not achievable in Earth based laboratories. In particular, the regions of space near compact objects or near the horizon of Black Holes are very likely particle acceleration sites. It is also possible (or perhaps likely) that the still unexplained cosmological Dark Matter will play an important dynamical role in precisely these acceleration sites (for example near the center of galaxies), and therefore one could have to disentangle the physics of particle acceleration and Dark Matter annihilation. In a nutshell: High Energy Astrophysics remains a crucial field for fundamental Science.

#### 4.3. Galactic to Extragalactic transition.

Berezinsky and collaborators<sup>25)</sup> have been the first to note the remarkable fact that the injection of a smooth (power law) spectrum of protons (with a sufficiently

---

<sup>i</sup> *A posteriori* it could be an interesting problem to consider why essentially the entire community of CR physicists has remained so “captured” with the idea of the existence of “super-GZK” particles” on the basis of an evidence of weak statistical significance and with the possibility of significant systematic errors. The “temptation” of the possible discovery of a result of extraordinary importance probably played a significant role for both observers and theorists.

small contributions of helium and other nuclei) can describe the UHCR not only above the “ankle” but in the entire energy range  $E \gtrsim 10^{18}$  eV. These authors stress the point that the prediction depends on only few parameters (the slope  $\alpha$ , the injection absolute normalization and the  $z$  dependence of its evolution) can provide a very good fit to the data, and have concluded that this is very unlikely to be a simple coincidence, and is evidence of a real effect.

The “Ankle” feature in the CR spectrum has been for a long time assumed to mark the transition energy where the softer galactic component is overtaken by the harder extragalactic one. In the Berezhinsky et al. model the flattening of the spectrum emerges from an entirely different physical mechanism. In the entire energy range, both above and below the “Ankle”, the spectrum is due to a single, proton dominated component, injected with a smooth (power law) spectrum. The visible structure in the spectrum is interpreted as the imprint of energy losses due to  $e^+e^-$  pairs production. This effects is mostly effective at an energy range around  $E \sim 10^{19}$  eV, and form a “dip” in the spectrum. The energy range of the effect is controled by the kinematical threshold for pair production at low energy, and by the fact that the energy lost for the production of an  $e^+e^-$  pair is  $\propto m_e^2/E$  decreases with  $E$ . The shape of the sprectrum distortion or “Dip” is in fact determined by simple, fundamental physics cosiderations and robustly predicted. The form of the spectrum is of course strongly dependent on the value of the slope  $\alpha$ . When the slope is  $\alpha \simeq 2.6$  (for no–evolution of the injection) or  $\alpha \simeq 2.4$  (for AGN/SFR source evolution) the spectral shape can describe the data in the entire energy range:  $[10^{18}, 10^{20}]$  eV,

The name “Dip model” encodes this new dynamical explanation and renames the structure traditionally called “Ankle”. In this model the transition between galactic and extra–galactic cosmic rays happens at lower energy and corresponds to the less prominent spectral steepening feature called “2nd–Knee”. For more discussion about observations of this structure see<sup>26)</sup>.

The “Dip Model” has attracted considerable interest, and is a leading contender for the description of the highest energy cosmic rays. In my view, the questions of where is the transition between galactic and extra–galactic cosmic rays, and if the “Ankle” is really a “Dip” or viceversa remain open, at the center of an important controversy, that will be soon settled by improved observations. The implications of this problem are important and wide.

If the “Dip Model” is correct, life for the observers would be significantly simplified. The reason is that it allows “calibrations” for the measurements of both energy and mass of the CR starting from  $E \sim 10^{18}$  eV. It is clearly possible to use an observed feature of the spectrum (with a well understood physical origin) to determine the scale of the energy measurements<sup>‡</sup>. In fact, the idea to use the “GZK suppres-

---

<sup>‡</sup>Matching the spectral shapes of different experiments one can estimate the *ratios* between their respective energy scales. To establish the absolute energy scale one obviously need to compare the observed spectra with a “template” based on an understood physical mechanism.

sion” to fix the CR energy scale is now 40 years old. In the “DIP model” one has a spectral feature (the “Dip”) that allows to play the same game at lower energy and with much higher statistics. Berezhinski and collaborators have already suggested corrections factors for the energy scale of the different UHECR experiment. It should be stressed that the validity of the “Dip Model” depends on the fact that the energy scale of the HiReS experiment is approximately correct, while the energy scale of the Auger experiment is significantly underestimated, as shown in fig. 5.

The same discussion can be made for the CR composition measurements. An established “GZK” feature implies a proton rich spectrum. In the “Dip Model” most particles above  $E \sim 10^{18}$  eV are protons. With this knowledge one can use the observations on the shower development to extract information on hadronic interactions at high energy (see discussion in section 7).

The relatively “soft” injection ( $\alpha = 2.4-2.6$ , depending on the assumptions about the source redshift evolution) of the “Dip model” is not expected in several acceleration models for both AGN’s and GRB’s that predict a slope closer to  $\alpha = 2$ . It should be noted however that the injection considered here is the space averaged one, and it is possible<sup>25)</sup> that the spectra of *individual* sources are all flatter (for example with  $\alpha \simeq 2$  but have different high energy cutoffs, that combine to an average spectrum that can be approximated with an effective softer power law. This explanation is however problematic, and it is unclear if it can naturally result in spectrum with the required smoothness.

The determination of the galactic/extra-galactic transition energy has obviously important consequences also for the properties of the galactic spectrum, and the galactic sources. In the models that have the transition at the “Ankle” it is necessary to assume that our own Galaxy contains sources capable to accelerate particles up to  $10^{19}$  eV and above. In the “Dip model” with a lower energy transition one has a less stringent (by a factor 10 of more) requirement for the maximum energy of the Milky Way accelerators.

The transition energy between galactic and extra-galactic cosmic rays obviously marks the passage from a softer to a harder component. It is therefore *natural* to expect that the transition appears as an *hardening* of the spectrum. The ‘Ankle’ is the only observed hardening of the spectrum, in the entire CR energy range, this has lead to its identification with the transition energy. In the Dip model the galactic to extra-galactic transition corresponds however to the “2nd-Knee”, that is to a spectral *steepening*. This may appear, and indeed it is surprising. The situation where the transition to a harder component *appears* as a softening is in fact possible but is requires the existence of two condition, that while perfectly possible are, in the absence of a dynamical explanation surprising coincidences:

1. Both galactic and extra-galactic components must have a steepening feature at approximately the same energy  $E^*$ . The extragalactic component must however

be the harder of the two, both below and above  $E^*$ .

2. At the energy  $E^*$  the two components must have approximately equal intensity ( $\phi_{\text{gal}}(E^*) \simeq \phi_{\text{extra}}(E^*)$ ).

Let us consider a situation where the galactic component has slopes  $\alpha_{\text{gal}}$  and  $\beta_{\text{gal}} > \alpha_{\text{gal}}$  below and above  $E^*$ , while the extragalactic component has slopes  $\alpha_{\text{extra}}$  and  $\beta_{\text{extr}} > \alpha_{\text{extra}}$ . If the relative normalization of the two component is “about right”, and if the 4 slopes are ordered as:

$$\alpha_{\text{extra}} < \alpha_{\text{gal}} < \beta_{\text{extra}} < \beta_{\text{gal}}$$

then one will observe a spectrum that steepens from the slope  $\alpha_{\text{gal}}$  to the slope  $\beta_{\text{extra}}$ , with the steepening marking the transition to the harder extra-galactic component. The two slopes  $\alpha_{\text{extra}}$  (extragalactic component below the transition) and  $\beta_{\text{gal}}$  (galactic component above the transition) are not easily measured because they are “hidden” by the dominant component.

The discussion above is just a toy model, but in fact it is also an approximation of what happens in the “Dip model”. At the transition energy (coincident with “2nd-Knee” at  $E^* \simeq 4 \times 10^{17}$  eV) one observes a spectrum softening from a slope  $\alpha \simeq 3.0$  to a slope  $\simeq 3.3$ . The spectrum below the knee reflects the shape of a more abundant galactic component ( $\phi_{\text{gal}} \propto E^{-3}$ ), while the harder ( $\phi_{\text{extra}} \propto E^{-2.4}$ ) extragalactic proton component is hidden below. Near the transition energy the galactic component two things happen: the galactic component steepens sharply (presumably because of the “end” of the galactic accelerators), while also the extragalactic component steepens because of the opening up of the pair production channel for energy loss, taking (just below the “2nd-Knee”) the approximate slope  $\sim 3.3$ . The relative normalization of the two components is such that one observes a single steepening transition (approximated as the slope transition  $3 \rightarrow 3.3$ ).

This situation is possible, but it is not *natural*, and seems to require some “fine tuning”. In fact the same critical observations have already been formulated in the past discussing the “knee” ( $E_{\text{knee}} \sim 3 \times 10^{15}$  eV) as a possible transition between two different CR populations. Additional discussion in support of the “Dip model” can be found in<sup>25)</sup> or<sup>29)</sup>.

In summary, the identification of the transition energy that separates galactic and extra-galactic cosmic rays is a central problem for high energy astrophysics, with wide and important implications.

Luckily it is likely that the problem will be solved with new observations especially those related to the mass composition and angular distribution of the cosmic rays. Essentially all CR models predict that the two components have very different mass composition (with a galactic component dominated by heavy nuclei, and an extragalactic one rich in protons), therefore the measurement of energy spectra

separately for different mass ranges has the potential to clearly disentangle the two components. Similarly, the large scale angular distribution of CR below and above the transition energy, (possibly also for different mass groups) can allow to separate an isotropic extra-galactic component from a galactic one that should show the effects of the Milky Way magnetic confinement.

#### 4.4. Energy Balance for Extra-Galactic CR

The average energy density of extra-galactic cosmic rays  $\rho_{\text{cr}}^{\text{extra}}$  is the result of the continuous injection of particles during cosmological history, taking into account the losses due to energy redshift and other interactions. Integrating over all energies and considering only redshift losses one has:

$$\rho_{\text{cr}}^{\text{extra}} = \int dt \frac{\mathcal{L}_{\text{cr}}(t)}{1+z(t)} = \int dz \frac{\mathcal{L}_{\text{cr}}(z)}{H(z)(1+z)^2} = \frac{\mathcal{L}_{\text{cr}}(0)}{H_0} f \quad (20)$$

where  $\mathcal{L}_{\text{cr}}(z)$  is the power density (in comoving coordinates) of the CR sources at the epoch  $z$  (and  $f \simeq 1 - -3$  is an adimensional quantity). Including pair and pion production losses for protons require a more complicated but straightforward analysis.

The estimate of the necessary CR power density is a very important constraint for the possible sources. This estimate is however difficult because only a small portion of the extragalactic spectrum is visible, with the low energy part hidden by the galactic foreground, and therefore the total energy density is not directly measured and can at best be obtained with an extrapolation based on theory.

It is possible to estimate the energy density (and correspondingly the power density) of cosmic rays above a minimum energy  $E_{\text{min}}$ . Fig. 6 plots the power density of the extragalactic proton sources that correspond to the fluxes given in fig. 4. All these fluxes reproduce the highest energy part (above the ‘‘Ankle’’) of the CR spectrum, but having different slopes they have different behaviours at lower energy. The required power density clearly depends on the minimum energy  $E_{\text{min}}$ , and is also a (rapidly varying) function of the slope  $\alpha$ .

The power density needed to generate the CR above  $10^{19}$  eV is of order:

$$\mathcal{L}_{\text{cr}}^0[E \geq 10^{19} \text{ eV}] \simeq (3 \div 6) \times 10^{36} \frac{\text{erg}}{\text{Mpc}^3 \text{s}}.$$

This power estimate depends only weakly on the assumed shape of the injection spectrum, however extrapolating to lower energy the power density increases slowly (logarithmically) for  $\alpha \simeq 2$  but faster ( $E_{\text{min}}^{\alpha-2}$ ) for softer injection. In the ‘‘Dip Model’’ where the CR injection is relatively soft ( $\alpha \gtrsim 2.4$ ) and the minimum energy is  $E_{\text{min}} \lesssim 10^{18}$  eV, one has a minimum power requirement  $\mathcal{L}_{\text{cr}}^0 \gtrsim 10^{38}$  erg/(Mpc<sup>3</sup>s), that is significantly larger than the previous estimate. If the power law form injection continues without break to lower energy, the power requirement increases with decreasing  $E_{\text{min}}$  and eventually becomes extraordinarily large.

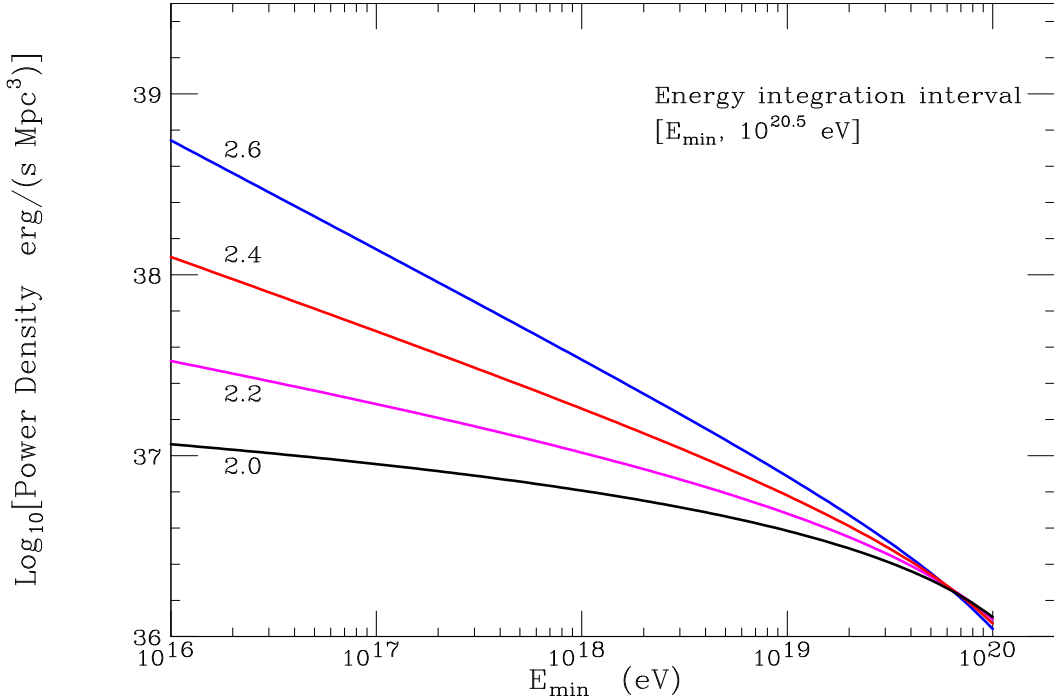


Figure 6: Power density necessary to produce the extra-galactic cosmic rays, plotted as a function of the minimum energy  $E_{\min}$  of the injected particles.

What are the possible candidates for the sources of the extragalactic CR, based on this power requirement? The two leading candidates are Active Galactic Nuclei (AGN) and Gamma Ray Bursts (GRB). The bolometric power density of the ensemble of AGN is uncertain but for example it was estimated by Ueda<sup>24)</sup> multiplying by a factor of 30 the observed energy density in hard X-ray ([10,20] KeV) band:

$$\mathcal{L}_{\text{AGN}}^{\text{bolometric}} \simeq 2 \times 10^{40} \left( \frac{\text{erg}}{\text{s Mpc}^3} \right) \quad (21)$$

It is not unreasonable to expect that a fraction of order 1–10% (or possibly more) of the released energy is transformed into relativistic particles, and therefore AGN satisfy the energy constraint.

Active Galactic Nuclei are the central regions of Galaxies that emit radiation in a very broad energy range, their source of energy is modeled as due the gravitational energy released in mass accretion on supermassive Black Holes (with mass as large as  $\sim 10^9$ – $10^{10} M_{\odot}$ ). It can be interesting to note that the power output of the ensemble of AGN can be checked against the observed mass density in supermassive Black Holes in the universe. When a mass element  $m$  falls into a Black Hole (BH) of mass  $M_{\bullet}$ , the BH mass increases by an amount  $\Delta M_{\bullet} \simeq (1 - \varepsilon) m$ , while the energy  $\varepsilon m$  is radiated away. The relation between a BH mass and the energy radiated during its

formation can therefore be estimated as:

$$M_{\bullet} = \frac{(1 - \varepsilon)}{\varepsilon} E_{\text{radiated}} \quad (22)$$

The radiation efficiency  $\varepsilon$  can be roughly estimated as the kinetic energy per unit mass ( $G M_{\bullet}/r$ ) gained by a particle falling into the BH potential down to a radius  $r$  equal to a few Schwarzschild radii ( $R_S = 2 G M_{\bullet}$ ), where the particle falls is temporarily arrested by the collision with the other accreting matter. For  $r \simeq 5 R_S$  one finds  $\varepsilon \sim 0.1$ . The measured density of BH's in the local universe<sup>30)</sup> is  $\rho_{\bullet} \simeq 4.6^{+1.9}_{-1.4} \times 10^5 M_{\odot}/\text{Mpc}^3$ , the corresponding density in radiated energy is of order  $\sim 10^{-4} \text{ eV}/\text{cm}^3$ , and if a fraction of few percent of this energy is converted into relativistic particles, this is sufficient to form the CR extragalactic spectrum.

The possibility to obtain sufficient power from Gamma Ray Bursts to fuel the observed extra-galactic cosmic ray density is the object of some dispute. Several authors<sup>32,33)</sup> have argued in favor of this explanation, while according to others (see for example<sup>29)</sup>) the GRB energy output is insufficient.

The long duration GRB's have been solidly associated with a subset of SN explosion. The SN blast waves are considered as the source of most of the galactic CR. The rate of SN explosions in the near universe is estimated<sup>31)</sup> as:

$$R_{\text{SN}}^{\text{observed}} \simeq 7.6^{+6.4}_{-2.0} \times 10^{-4} (\text{Mpc}^{-3} \text{ yr}^{-1}) \quad (23)$$

in good agreement with theoretical estimates based on the star formation (and death) rates. This SN rate corresponds to the power density (in the form of kinetic energy of the ejecta)  $\mathcal{L}_{\text{SN}}^{\text{kin}} \simeq 3 \times 10^{40} \text{ erg}/(\text{Mpc}^3\text{s})$ , and presumably to a CR power density 5–10 times smaller. It is however assumed that most of the CR produced around the spherical SN shocks cannot reach the energy range where the extragalactic CR are visible. The GRB phenomenon, that is the emission of ultrarelativistic jets is associated with a small fraction of the GRB, estimated by Woosley and Hower<sup>34)</sup> as less than 1% the core collapse SN. Estimating a CR emission energy per GRB of order  $10^{51} \text{ erg}$  this can provide a CR injection power density of order  $10^{37}\text{--}10^{38} \text{ erg}/(\text{Mpc}^3\text{s})$ . This is sufficient to generate the extragalactic CR in models where the injection has a flat spectrum, or where the CR emission is limited to very high energy, but it is likely to be too small for other models with softer injection, and an emission that grows to  $E$  as small as a TeV or less.

## 5. Cosmic Ray Point Sources

At a sufficiently high energy the magnetic deviations of charged particles in the propagation from their sources should become sufficiently small so that it becomes possible to perform high energy cosmic ray astronomy. This simple and very attractive idea has been for a long time a “dream” for CR physicists and, with a high degree of

confidence, has recently become a reality thanks to new data of Auger<sup>35,36</sup>, even if the result has received only weak or no confirmation by the Yakutsk<sup>37</sup>) and HiRes<sup>38</sup>) detectors, and the interpretation of the result remains controversial, at the center of very lively discussion.

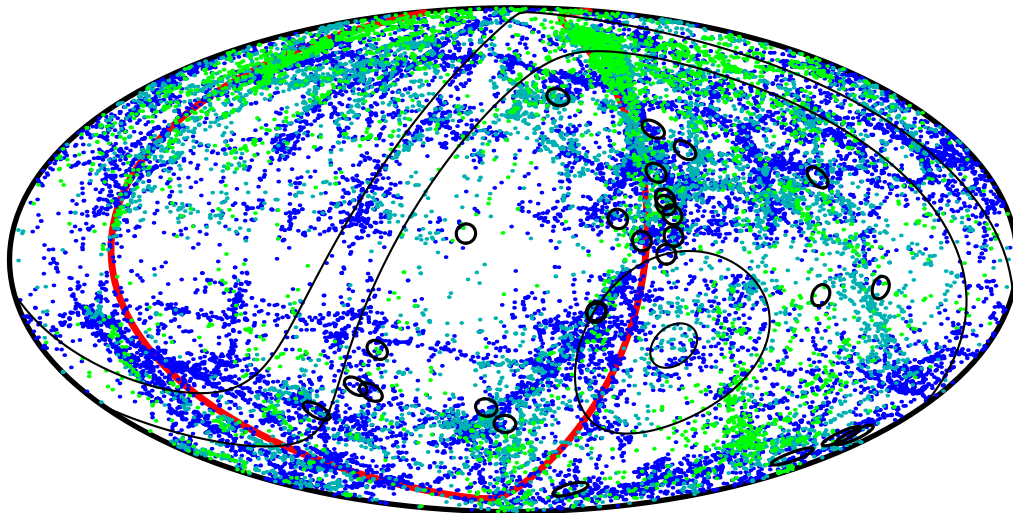


Figure 7: Hammer–Aitoff (equal area) projection of the Auger (black circles) events with energy  $E \geq 6 \times 10^{19}$  eV. The points are galaxies with  $z < 0.015$ . The thick (red) line is the so called “Super-Galactic plane”. The thin lines delimit regions in the sky that have received equal exposures.

For quasi-linear propagation, the angular deviation of a charged particle propagating for a distance  $d$  in extragalactic space can be estimated assuming that the field has a typical value  $B$ , and it is organized in “magnetic domains” of linear size  $\lambda_B$  where the field direction roughly parallel. Summing the deviations contributed by all magnetic domains crossed by a particle results in the estimate of the deviation:

$$(\delta\theta)^2 \simeq N_{\text{domains}} \left( \frac{\lambda_B}{r_L} \right)^2 = \frac{d \lambda_B (Z e B)^2}{E^2} \quad (24)$$

(where  $r_L = E/(Z e B)$  is the Larmor radius). Numerically:

$$\delta\theta = 0.53^\circ Z B_{\text{nG}} \sqrt{(d \lambda)_{\text{Mpc}}} \left( \frac{10^{20} \text{ eV}}{E} \right) \quad (25)$$

Astronomy with CR of energy  $E$  is therefore possible (for an angular resolution of order  $\delta\theta$ ) only within a sphere of radius:

$$R_{\text{imaging}}(E, \delta\theta) = \frac{E^2 \delta\theta^2}{(Z e B)^2 \lambda_B} \quad (26)$$

The “CR imaging radius” is strongly dependent ( $\propto E^2/Z^2$ ) from the charge and energy of the particle considered, and shrinks also rapidly ( $\propto (\delta\theta)^2$ ) if one requires

sharper images. The crucial parameter that fixes the size of the CR imaging sphere is the combination  $(B^2\lambda_B)^{-1}$  that characterizes the extragalactic magnetic field.

At the end of 2007 the Auger collaboration<sup>35,36)</sup> has published some potentially very important results about the angular distribution of their highest energy events. The Auger group has shown that the arrival directions of the 26 highest energy events ( $E_{\min} \simeq 57 \times 10^{18}$  eV), and the positions of the closest 292 Active Galactic Nuclei contained in the Veron Cetty catalogue, and in the detector field of view with a maximum redshift  $z_{\max} = 0.017$  (corresponding to  $d \lesssim 71$  Mpc) are correlated. Of the 26 selected events, 20 arrive within a cone of aperture  $\psi = 3.2^\circ$  around one of the AGN positions. The expected number of coincidences for an isotropic distribution of the CR arrival direction is estimated as 5.6, and the significance of the excess, taking into account the “statistical cost” of optimizing the three quantities  $\{E_{\min}, z_{\max}, \psi\}$  is estimated<sup>k</sup> as  $P = 1.7 \times 10^{-3}$ .

This important result has attracted considerable attention and several comments have already appeared in the literature. The most straightforward (or “naive”) interpretation of the results is of course that the AGN themselves are the sources of the highest energy CR, and that the angular scale of  $3.2^\circ$  is simply the typical deviation suffered by the particles during their propagation from their sources. This would be an extraordinary result that at the same time (a) solves (or goes a very long way toward solving) the problem of the UHECR sources; (b) gives a crucial measurement of the properties of the extragalactic magnetic field; and more controversially (c) measure the electric charge ( $Z \simeq 1$ ) of the UHECR. It should be noted that the angular resolution of the Auger detector is better than  $1^\circ$ , and therefore the 3 degrees cone is not a physical, and not an instrumental effect. This deviation is accumulated during the entire trajectory of the particle, and can be decomposed in contributions from the “source envelope”, the extragalactic propagation and finally deviations in the Milky Way disk and magnetic halo.

$$(\delta\theta) \simeq (\delta\theta)_{\text{source}} \oplus (\delta\theta)_{\text{extra}} \oplus (\delta\theta)_{\text{MW halo}} \oplus (\delta\theta)_{\text{MW disk}} \quad (27)$$

Our knowledge of the large scale of the magnetic field of our own Galaxy especially away from the disk is incomplete and non-precise, however it is reasonable to expect that for the energies considered the integral of the magnetic field  $\int d\vec{\ell} \vec{B}(\ell)$  over most line of sights corresponds to deviations larger than  $3^\circ$  if the charge much larger than unity, and therefore one can use our own galaxy as a spectrometer to determine that the CR are protons or at most light nuclei. Interpreting the dimension of the cone that optimizes the correlation with the AGN as the deviation angle of the particles one can also use equation (24). for a first estimate of  $B^2\lambda_B$ . Inserting the values

---

<sup>k</sup>This probability is estimated in robust way, “optimizing” the three parameters from only the first half of the collected data, and then computing  $P$  from the second half of the data, keeping the parameters fixed

$\delta\theta = 3.1^\circ$ ,  $d \simeq 71$  and  $E = 60 \times 10^{19}$  eV in (24) one obtains:

$$Z^2 B^2 \lambda_B \simeq 0.15 \text{ (nGauss)}^2 \text{ Mpc} \quad (28)$$

(where  $Z \sim 1$  is the charge of the observed particles). This implies an imaging radius:

$$R_{\text{imaging}} = 210 \left( \frac{E}{10^{20} \text{ eV}} \right)^2 \left( \frac{\delta\theta_{\text{image}}}{3^\circ} \right)^2 \text{ Mpc} \quad (29)$$

that is very encouraging for the perspectives of CR astronomy.

These “nominal” interpretation of the Auger data has however a number of significant problem and it can only considered as tentative. In fact the publications of the Auger group are very careful in observe that since the AGN distribution is correlated to the distribution of normal galaxies. Moreover, the Auger data can can also be interpreted<sup>39,40)</sup> assuming that the anisotropy the effect is mostly due to the a the contribution of a single source, the nearby ( $d \simeq 3.5$  Mpc) Active Galactic Nucleus CEN A, generating as much as one third of the events above  $6 \times 10^{19}$  eV, with a larger angular spread of order  $\delta\theta \simeq 10^\circ$  (or more). Substituting the shorter distance and the larger  $\delta\theta$  one obtains an estimate of  $B^2 \lambda_B$  larger by a factor of order 200:

$$Z^2 B^2 \lambda_B \simeq 42 \text{ (nGauss)}^2 \text{ Mpc} \quad (30)$$

and correspondingly a 200 times smaller imaging radius. The discrimination between the two estimates (28) and (30) for the parameter that describes the extragalactic magnetic field is obviously crucial for the future of the field.

## 6. Cosmic Ray Composition and Hadronic Interactions

A crucial problem for CR science is the estimate of the energy and mass of the detected particles. At high energy it is only possible to observe the showers produced in the atmosphere by CR particles, and to extract information about the properties of the primary particle it is obviously necessary to have a sufficiently accurate description of the shower development. The key ingredient, and the dominant source of systematic uncertainty is the description of the properties of hadronic interactions, such as: cross sections, final state multiplicities and inclusive energy spectra. At a fundamental level there are few doubts that Quantum–Chromo–Dynamics (QCD) is a complete and successful theory of the strong interactions; however the fundamental fields that enter the QCD Lagrangian are only quarks and gluons, and perturbative calculations are only possible for high momentum transfer processes between these fields. Most of the observables that are relevant for shower development cannot be calculated from first principles. These quantities (like cross sections and multiplicities) must be obtained from measurements obtained in accelerator experiments. The difficulty here is that the available data do not entirely cover the relevant phase space, and

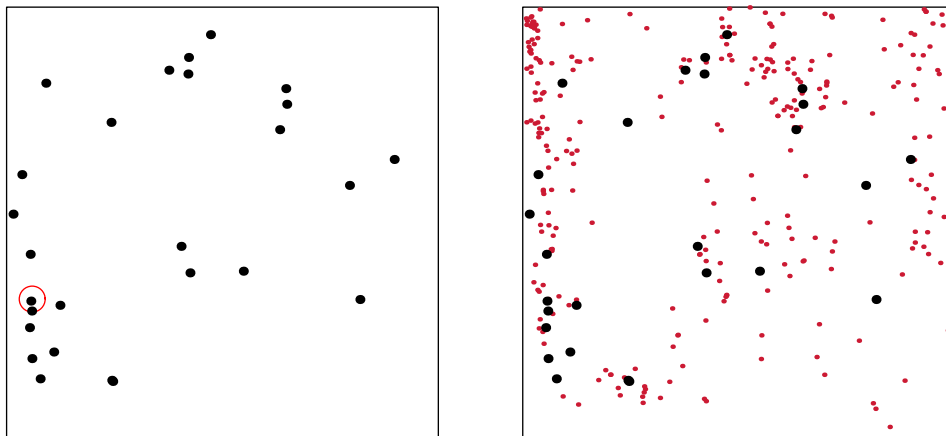


Figure 8: The left panel shows the angular distribution of the 26 highest energy events of Auger<sup>35</sup>). The horizontal  $x$  axis corresponds to the right ascension and the vertical  $x$  axis to the declination  $\delta$ . The  $y$  coordinates have been “stretched” taking into account the declination dependence of the exposure, so that for an isotropic distribution, the points that correspond to the measured directions should fill uniformly the square. The probability that the measured arrival directions are distributed uniformly is few percent. The right panel shows the distribution of near ( $z < 0.015$ ) AGN in the Veron–Cetty catalogue. The position of CEN A is also shown as a red circle in the left panel.

therefore for the interpretation of CR observations it is necessary to *extrapolate* from the regions where observations are available, using guidance from the known structure of the underlying theory.

The incomplete phase space coverage is evident if we consider the center of mass energy of the first CR interaction, that for the highest energy particles with  $E \sim 10^{20}$  eV is  $\sqrt{s} \sim 430$  TeV, four hundred times larger than the highest energy where accelerator data is available (at the  $p\bar{p}$  Tevatron collider). This “energy gap” will be only partially filled by the eagerly awaited data of the LHC collider at CERN with a c.m. energy  $\sqrt{s} = 14$  TeV (see for example a plot of the total  $pp$  cross section in fig. 9). It should also be noted that data at high  $\sqrt{s}$  is available only for  $pp$  or  $p\bar{p}$  collisions, (and not for meson–nucleon and hadron–nucleus interactions). Note also that for an accurate description of the shower development it is necessary to have a precise description of the highest energy secondaries (in the projectile fragmentation region), these particles are experimentally the most difficult to measure in collider experiments, and significant uncertainties about their energy spectrum still exist. For this reason even below the knee ( $\sqrt{s} \simeq 2.3$  TeV) uncertainties in the description of the hadronic interactions are a source of significant errors in the energy and mass measurement.

Fortunately, the uncertainties in the description of hadronic interactions play only a limited role in the energy determination for the highest energy particles, where one can observe showers using the fluorescence light method pioneered by the Fly’s Eye detector. Relativistic charged particles in air excite nitrogen molecules in the medium.

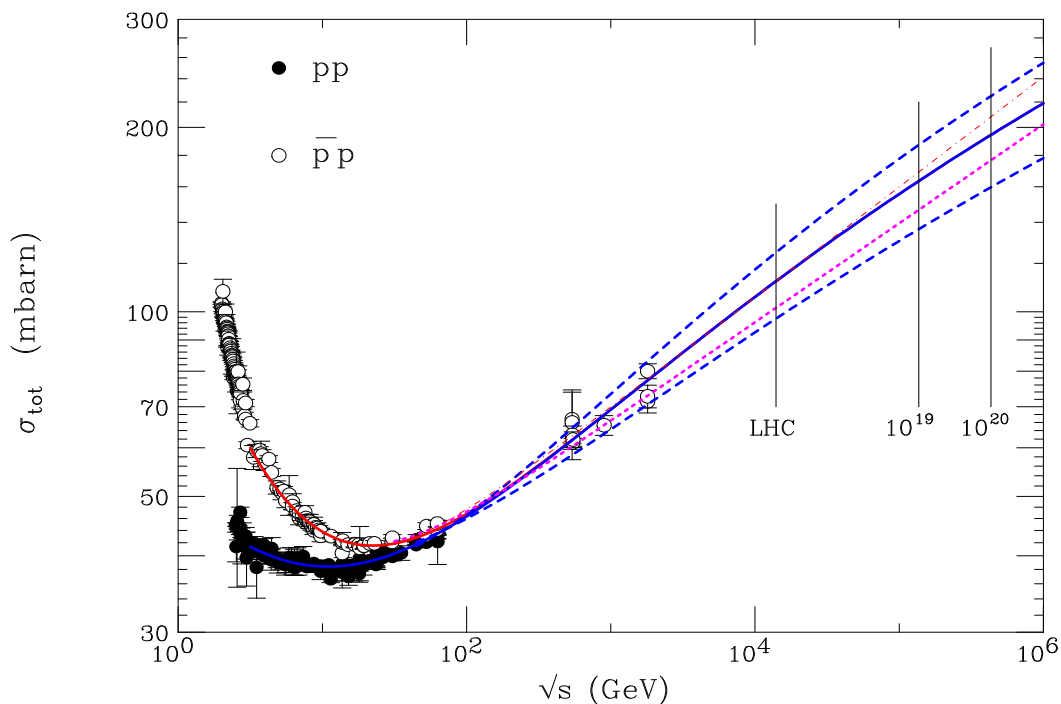


Figure 9: Total cross sections for  $pp$  and  $\bar{p}p$  scattering. The filled (empty) points are measurements for the  $pp$  ( $\bar{p}p$ ) channel. The solid line is a result of a fit in <sup>41)</sup> The dotted line is the fit in <sup>42)</sup>

These excited molecules can return to the fundamental states emitting isotropically fluorescence photons, that are detectable at the ground, with the shower appearing as a quasi point-source of light moving at the speed of light across the sky. The photon emission is proportional to the number of charged particles, and therefore from the angular distribution of the detected photons it is possible to reconstruct the longitudinal profile  $N_e(X)$  of each detected shower<sup>1</sup>. The longitudinal profile  $N_e(X)$  allows the model independent reconstruction of the energy dissipated in air by the shower as ionization (and then ultimately heat):

$$E_{\text{ionization}} = \int_0^{X_{\text{ground}}} dX \left\langle \frac{dE}{dX} \right\rangle N_e(X) \quad (31)$$

The total shower energy can be calculated adding to this dominant contribution smaller correction terms that take into account the energy that goes into neutrinos, muons, and is dissipated in other (as hadronic and electromagnetic components) below the ground:

$$E_{\text{shower}} = E_{\text{ionization}} + E_{\nu} + E_{\mu} + E_{\text{ground}} \quad (32)$$

<sup>1</sup>  $N_e$  is the number of charged particles present at the depth  $X$ , and the column density  $X$  can be used as a coordinate along the shower axis

The correction terms  $E_\nu$ ,  $E_\mu$  and  $E_{\text{ground}}$  are mass and model dependent, but fortunately account for a small fraction (of order  $\sim 10\%$ ) of the primary particle energy, and the energy measurement has only a small model dependence.

In other words, according to equation (31), the *area* subtended by the longitudinal profile  $N_e(X)$  is a measurement of the shower energy that is independent from the particle type and from the modeling of hadronic interactions; on the other hand the *shape* of the curve depends on both the primary particle mass and the properties of hadronic interactions.

The shape of the showers longitudinal development is in fact the best available method to estimate the mass of UHECR. It is in fact intuitive that, for the same total energy, the showers generated by a nucleus of mass  $A$  will develop more rapidly, reaching their maximum size at a shallower depth. Because of fluctuations this method cannot identify the mass of an individual shower, but can be used statistically to estimate the mass composition at a given energy. The simplest method is to use the average value  $\langle X_{\text{max}}(E) \rangle$  of the position of maximum size for all showers with energy  $E$  as a measurement of the average mass of CR at that energy.

For a more quantitative analysis one can denote  $X_{\text{max}}^p(E)$  the average position of shower maximum for proton showers and, since showers penetration grows approximately logarithmically with increasing energy, develop in first order around energy  $E^*$ . Measuring the energy in units of  $E^*$  one obtains:

$$X_{\text{max}}^p(E) \simeq \overline{X}_p(E^*) + D_p \ln E \quad (33)$$

The quantity  $D_p$  gives the increase in the average position of shower maximum when the  $p$  energy increases by a factor  $e$  and is known as the proton “elongation rate”

To a very good approximation the quantity  $X_{\text{max}}^A(E)$ , that is the average position of maximum for showers generated by a primary nucleus of mass  $A$  and total energy  $E$  is related to the average maximum for proton showers by the relation:

$$X_{\text{max}}^A(E) \simeq X_{\text{max}}^p\left(\frac{E}{A}\right) \simeq X_{\text{max}}^p(E) - D_p \ln A \quad (34)$$

In (34) the first equation is clearly correct for a naive superposition model (where the shower generated by a nucleus containing  $A$  nucleons is described as the superposition of  $A$  nucleon showers each having energy  $E/A$ ), but in fact it has a much more general validity<sup>45)</sup>, since it is based on the relations between the cross sections for nuclei and nucleons in the framework of the Glauber model<sup>46)</sup>; the second equality in (34) follows from (33).

More in general, if the CR of energy  $E$  are a mixture of nuclei with different mass  $A$ , the average  $\langle X_{\text{max}} \rangle$  can be expressed as:

$$\langle X_{\text{max}}(E) \rangle \simeq X_{\text{max}}^p(E) - D_p(E) \langle \ln A \rangle_E \simeq \overline{X}_p + D_p [\ln E - \langle \ln A \rangle_E] \quad (35)$$

where  $\langle \ln A \rangle_E$  the average value the logarithm of  $A$  for particles of energy  $E$ . One can then use equation (35) to estimate the mass composition of UHECR comparing the measured  $\langle X_{\max} \rangle$  with the value expected theoretically for protons:

$$\langle \ln A \rangle_E = \frac{\langle X_{\max}(E) \rangle - X_p(E)}{D_p} \quad (36)$$

Similarly comparing the experimental elongation rate  $D_{\text{exp}} = d\langle X_{\max}(E) \rangle / d \ln E$  with the elongation rate for protons (or nuclei)  $D_p$ , one can estimate the rate of variation of the composition with energy:

$$\frac{d\langle \ln A \rangle_E}{d \ln E} = 1 - \frac{D_{\text{exp}}}{D_p} \quad (37)$$

An illustration of the present situation of the mass composition of UHECR is shown in fig. 10. The points in the figure show the average  $X_{\max}$  for UHE showers obtained by the HiRes–MIA<sup>48)</sup>, HiRes<sup>47)</sup> and Auger<sup>49)</sup> experiments. The thick lines are fit to the data points obtained by the experimental groups. while the thin lines in the figure are theoretical predictions calculated assuming a pure composition of only protons or only iron nuclei based on the hadronic models of Sibyll<sup>43)</sup> and QGSJET<sup>44)</sup>. At face value these results seems to indicate that the UHECR are not pure protons nor pure iron nuclei, but are a combination (with approximately equal weight) of the two species, or are mostly nuclei of intermediate mass. This conclusion however relies on the assumptions that the models used for the description of the hadronic interaction are at least approximately correct.

The composition of the CR has very important consequences for the properties of their acceleration sites, and therefore it is of great importance to gain a more robust understanding of the relevant properties of hadronic interactions, and a better estimate of the systematic uncertainties. It is clear for example that if the cross section is larger or if the energy spectra of the final state particles are softer than what is assumed in the theoretical prediction, the real showers develop faster than the simulated ones, and the composition interpretation is biased in the direction of a too heavy composition.

In the discussion of the previous paragraph, information about elementary particle physics (obtained from accelerator experiments) is used to measure the mass composition of the highest energy CR, and then infer the structure and properties of their astrophysical sources. It is interesting that this “logical flow” can be in principle be “inverted”. In fact there are (at least in principle) methods to measure the composition of CR that are independent from the detailed properties of their showers. These methods, as discussed above, are based on essentially two ideas: (i) the “cosmic magnetic spectrometer”, and (ii) the imprints of energy losses on a smooth injection spectrum. If the “nominal interpretation” of the Auger anisotropy analysis<sup>35)</sup> is correct and the deviations of extragalactic particles with  $E \sim 6 \times 10^{19}$  eV is as small

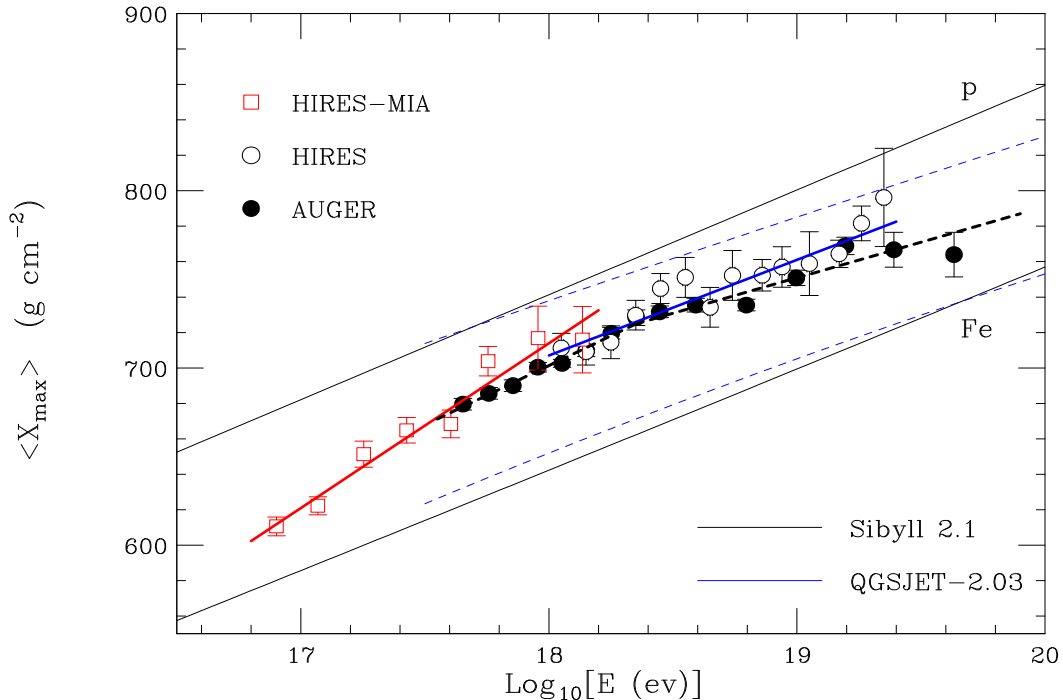


Figure 10: Measurements of  $\langle X_{\max} \rangle$  obtained by the HiRes-MIA <sup>48)</sup>, HiRes <sup>47)</sup> and Auger <sup>49)</sup> experiments. The lines are montecarlo calculations for protons ( $p$ ) and iron nuclei (Fe) performed using the SIBYLL <sup>43)</sup> and QGSJET <sup>44)</sup> interaction models.

as  $3^\circ$  their electric charge is in fact strongly constrained, by our (however still poor) knowledge of the galactic magnetic fields. Similarly, if the “Dip Model” of Berezhinsky and collaborators <sup>25)</sup> is correct and the structure of the ankle corresponds to the effects of  $e^+e^-$  pairs production in  $p\gamma$  interactions, then the identity of the UHECR particles is determined. In this case, the requirement of consistency for the penetration of the corresponding showers can be used to obtain information about the properties of hadronic interactions.

## 7. Outlook

The observation and understanding of the “High Energy Universe” is one of the important frontiers of fundamental Science. Our universe contains astrophysical objects that are capable to accelerate particles to ultrarelativistic energies as large as  $\sim 10^{20}$  eV. The nature and structure of these cosmic accelerators and the physical mechanism that are operating in them are beginning to be clarified, even if large uncertainties still exist. In fact, several classes of these cosmic accelerators are now known to exist. There is good evidence that hadronic particles (protons and nuclei) are accelerated in SuperNova Remnants and Active Galactic Nuclei, while electrons/positrons are also efficiently accelerated in several other environments like pulsars and pulsars

wind nebulae. Gamma Ray Bursts are also clearly sites of particle acceleration. These extraordinary environments are very important astrophysical laboratories to test our physical theories.

The acceleration of charged particles is unavoidably connected to the radiation of photons and (in the case of hadronic particles) to the emission of neutrinos. Moreover many of these accelerators are connected to the violent motion of large masses and to the possible emission of gravitational waves. Therefore the complete study of these objects must rely on the combined use of different “messengers” (photons in a very broad range of wavelength, cosmic rays, neutrinos and gravitational waves). We are now witnessing the opening of new “astronomies” with cosmic ray particles (at sufficiently high energy to reduce the bending by magnetic fields), neutrinos and gravitational waves. The nearby active galactic nucleus Cen A is very likely the first astrophysical objects imaged with charged particles. The development of multi-messenger astronomy is a revolution comparable to the use of the telescope for astronomical observations started by Galileo in 1609, nearly exactly four centuries ago, and is certainly going to produce exciting results.

## 8. Acknowledgements

I would like to acknowledge discussions with Ralph Engel, Tom Gaisser, Maurizio Lusignoli, Todor Stanev and Silvia Vernetto. Many thanks to Milla Baldo Ceolin for the organization of another very fruitful workshop.

## 9. References

- 1) R. Abbasi *et al.* [HiRes Coll.], arXiv:astro-ph/0703099.
- 2) M. Roth [Pierre Auger Coll.], arXiv:0706.2096 [astro-ph].
- 3) K. Greisen, Phys. Rev. Lett. **16**, 748 (1966).  
G. T. Zatsepin & V. A. Kuzmin, JETP Lett. **4**, 78 (1966).
- 4) P. Sreekumar *et al.*, Phys. Rev. Lett. **70**, 127 (1993).
- 5) J.J. Engelmann *et al.*, Astron. Astrophys. **233**, 96 (1990).
- 6) J.J. Connell, Ap.J. **501**, L59 (1998).
- 7) Walter Baade & F. Zwicky, Phys. Rev. **45**, 138 (1934).
- 8) V. L. Ginzburg & S.I.Syrovatskii, “The origin of cosmic rays”, New York (1969)
- 9) L.O.C.Drury, Rep. Prog. Phys. **46**, 973 (1983).
- 10) E. Fermi, Phys. Rev. **75**, 1169 (1949).
- 11) HESS Coll., Nature **432**, 75 (2004) [arXiv:astro-ph/0411533].
- 12) HESS Coll., Astr. Astroph. **464**, 235 (2007) [arXiv:astro-ph/0611813].
- 13) MAGIC Coll., Astr. Astroph. **474**, 937 (2007) arXiv:0706.4065 [astro-ph].
- 14) A.De Rujula, Nucl.Phys.Proc.Suppl. **165**, 93 (2007) [arXiv:hep-ph/0608092].
- 15) A. Dar & A. De Rujula, arXiv:hep-ph/0606199. .

- 16) A. Dar & A. De Rujula, Phys. Rept. **405**, 203 (2004) [astro-ph/0308248].
- 17) T. Piran, Rev. Mod. Phys. **76**, 1143 (2004) [astro-ph/0405503].
- 18) B. Zhang & P. Meszaros, Int. J. Mod. Phys. A **19**, 2385 (2004) [astro-ph/0311321].
- 19) A. Dar & A. De Rujula, arXiv:hep-ph/0611369.
- 20) P. Lipari, Nucl. Instrum. Meth. A **567**, 405 (2006) [arXiv:astro-ph/0605535].
- 21) F. Vissani, Astropart. Phys. **26**, 310 (2006) [arXiv:astro-ph/0607249].
- 22) KASCADE Coll., Astropart. Phys. **24**, 1 (2005) [arXiv:astro-ph/0505413].
- 23) A. M. Hillas, Ann. Rev. Astron. Astrophys. **22**, 425 (1984).
- 24) Y. Ueda *et al.*, Prog.Th.Phys.Supp **155**, 209 (2004).
- 25) V. Berezhinsky, A. Z. Gazizov & S. I. Grigorieva, Phys. Lett. B **612**, 147 (2005) [arXiv:astro-ph/0502550].
- 26) D.R.Bergman & J.W.Belz, J. Phys. G **34**, R359 (2007).
- 27) M. Amenomori *et al.* [TIBET III Collaboration], arXiv:0801.1803 [hep-ex].
- 28) A. M. Hillas, J. Phys. G **31**, R95 (2005).
- 29) A. M. Hillas, arXiv:astro-ph/0607109.
- 30) A.Marconi *et al.* MNRAS **351** , 169 (2004) [astro-ph/0409542].
- 31) M.Fukugita & P.J.E. Peebles, Astroph. J. **616**, 643 (2004).
- 32) C. D. Dermer, arXiv:0711.2804 [astro-ph].
- 33) M. Vietri, D. De Marco & D. Guetta, Astrophys. J. **592**, 378 (2003) [arXiv:astro-ph/0302144].
- 34) S. E. Woosley, A. Heger & T. A. Weaver, Rev. Mod. Phys. **74**, 1015 (2002).
- 35) Auger Coll., Science **318**, 938 (2007) [arXiv:0711.2256 [astro-ph]].
- 36) Auger Coll., Astropart. Phys. **29**, 188 (2008) [arXiv:0712.2843 [astro-ph]].
- 37) Yakutsk collaboration, Pisma Zh. Eksp. Teor. Fiz. **87**, 215 (2008) [JETP Lett. **87**, 185 (2008)] [arXiv:0803.0612 [astro-ph]].
- 38) R. U. Abbasi *et al.*, arXiv:0804.0382 [astro-ph].
- 39) D.S.Gorbunov *et al.*, arXiv:0804.1088 [astro-ph].
- 40) T. Stanev, arXiv:0805.1746 [astro-ph].
- 41) J. R. Cudell *et al.* [COMPETE Coll.], Phys. Rev. Lett. **89**, 201801 (2002) [arXiv:hep-ph/0206172].
- 42) A. Donnachie & P. V. Landshoff, Phys. Lett. B **296**, 227 (1992)
- 43) R. S. Fletcher *et al.*, Phys. Rev. D **50**, 5710 (1994).
- 44) S. Ostapchenko, [arXiv:0706.3784 [hep-ph]].
- 45) R. Engel, T. K. Gaisser, P. Lipari & T. Stanev, Phys. Rev. D **58**, 014019 (1998) [arXiv:hep-ph/9802384].
- 46) R. J. Glauber & G. Matthiae, Nucl. Phys. B **21**, 135 (1970).
- 47) HigRes Coll., Astroph. J. **622**, 910 (2005) [arXiv:astro-ph/0407622].
- 48) HiRes-MIA Coll., Astroph. J. **557**, 686 (2001) [arXiv:astro-ph/0010652].
- 49) Auger Coll., arXiv:0706.1495 [astro-ph].